Digest Journal of Nanomaterials and Biostructures Vol. 5, No 4, October-December 2010, p. 959-973

NOVEL PORPHYRIN-BASED POLYSILOXANE MICROMATERIAL

S. GRAMA[a], N. HURDUC[a], E. FAGADAR-COSMA[b],
M. VASILE[c], E. TARABUKINA[d], G. FAGADAR-COSMA[e*]
[a]*Technical University «Gheorghe Asachi» Iasi, Department of Natural and Synthetic Polymers, Mangeron Ave No. 73, 700050-Iasi, Romania*
[b]*Institute of Chemistry Timisoara of Romanian Academy, M. Viteazul Ave, No. 24, 300223-Timisoara, Romania*
[c]*National Institute for Research and Development in Electrochemistry and Condensed Matter, P. Andronescu Street, No. 1, 300224- Timisoara, Romania*
[d]*Institute of Macromolecular Compounds, Russian Academy of Sciences, Bolshoy prosp. 31, 199004 St.-Petersburg, Russia*
[e]*"Politehnica" University of Timisoara, Piata Victoriei No. 2, 300006-Timisoara, Romania*

A new porphyrin modified polymer by the nucleophilic substitution at the chlorobenzyl groups on the side-chain of a polysiloxane with an asymmetrical mono-hydroxy-functionalized porphyrin, namely: 5-(4-hydroxyphenyl)-10,15,20-triphenyl-porphyrin is reported. The porphyrin-containing polysiloxane was characterized by ^{1}H-NMR and FT-IR spectroscopy and thermal analysis (DSC and thermo-gravimetric), the obtained data confirming the porphyrin connection on the polysiloxanic chain and showing an increased thermal stability of the modified polymer. A comparison between optical absorption spectroscopy data and emission spectra of the bare porphyrin and of the polymer shows that the porphyrin-base polysiloxane preserves the optical properties of the porphyrinic dye. Atomic force microscopy (AFM) put into evidence a spongeous structure of the functionalized polysiloxane material, with uniformly dispersed globular pores, a topography that encourages to further application of this material in formulation of sensor devices.

(Received October 2, 2010; accepted October 27, 2010)

Keywords: Polysiloxanes, Porphyrins, Fluorescence, Microstructures, Thermal properties

1. Introduction

The chemistry and technology of siloxane-based polymers, or silicones, is a very broad and still growing research area. As the most stable polymer available, silicones offer superior reliability, god service life and reduced production costs. Due to their excellent properties (low glass transition temperature, very low surface energy, gas permeability, resistance to oxidation and ultraviolet light, biocompatibility, etc.) this class of polymers lead to materials which have been investigated for a wide range of potential applications: surfactants, biomaterials, membranes, adhesives, electrical insulator, cosmetics etc. [1]. The siloxane bond particularity has a great impact concerning the polymer applications. The Si-O bond distance, shorter than the sum of covalent radii, implies a partial double bond character of Si-0. Nevertheless the barrier of rotation around the Si-0 bond is very low (ca. 2.5 kJ mol) the polymer chain having a very high flexibility [2]. The silicone materials may be conveniently grouped into products based upon fluids, cross-linked elastomers and resins [3]. Modifications of polysiloxane are extensively explored in order to obtain special properties thus giving access to new applications. Polydimethylsiloxanes in

---

[*] Corresponding author: gfagadar@yahoo.com

which some methyl groups are replaced by reactive organo-functional ones are now widely used in order to obtain new organic-silicone architectures [4-7]. If the reactive group is situated in the side-chain, materials with self-assembly properties can be obtained [8, 9].

As a consequence of these results, extended research has already performed to bind in a covalent way porphyrins, because of their amazing optical [10] electrical [11] and catalytic properties [12], onto different types of polymers [13-15].

Porphyrin-based covalently linked polymers preserve the initial properties of chromophore dye and can find possible application in the photodynamic therapy of cancer [16] as well as in the formulations for gas sensing [17], as a source of free charge carriers [18] or in conducting polymer devices [19].

The present study reports the obtaining of a new porphyrin modified polymer by the nucleophilic substitution of the chlorobenzyl groups on the side-chain of a polysiloxane with an asymmetrical mono-hydroxy-functionalized porphyrin, namely: 5-(4-hydroxyphenyl)-10,15,20-triphenyl-porphyrin (THPP). The porphyrin-containing polysiloxane was characterized by ^{1}H-NMR and FT-IR spectroscopy and thermal analysis (DSC and thermo-gravimetric), the obtained data confirming the porphyrin connection on the polysiloxanic chain and showing an increased thermal stability of the modified polymer. A comparison between optical absorption spectroscopy data and emission spectra of the bare porphyrin and of the polymer shows that the porphyrin-base polysiloxane preserves the optical properties of the porphyrinic dye. Atomic force microscopy (AFM) put into evidence a spongeous structure of the functionalized polysiloxane material, with uniformly dispersed globular pores, a topography that encourages to further application of this material in formulation of sensor devices.

2. Experimental

The synthesis of 5-(4-hydroxyphenyl)-10,15,20-triphenyl-porphyrin (THPP) was done by multicomponent method Adler-Longo (Scheme 1), according to improved literature data [20-24], and fully characterized by ^{1}HNMR, UV-vis, FT-IR, fluorescence excitation and emission spectra, MS, HPLC and TLC.

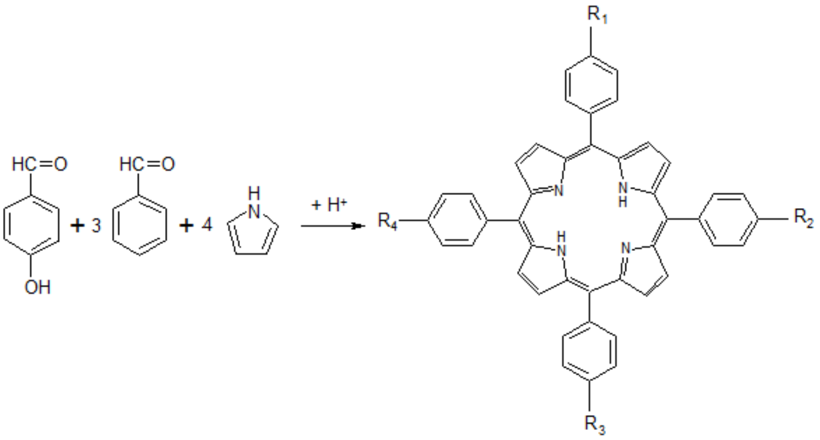

Scheme 1. The general equation for multicomponent synthesis of 5-(4-hydroxyphenyl)-10,15,20-triphenyl-porphyrin (THPP)

R_1=R_2=R_3=R_4=H, namely: 5,10,15,20-tetrakis-phenyl-porphyrin;
R_1=R_2=R_3=H; R_4=OH, namely: 5-(4-hydroxyphenyl)-10,15,20-triphenyl-porphyrin;
R_1=R_2=H; R_3=R_4=OH, namely: 5,10-di(4-hydroxyphenyl)-15,20-diphenyl-porphyrin (*cis*);
R_1=R_3=H; R_2=R_4=OH, namely: 5,15-di(4-hydroxyphenyl)-15,20-diphenyl-porphyrin (*trans*);
R_1=R_2=R_3=OH; R_4=H, namely: 5,10,15-tri(4-hydroxyphenyl)-20-phenyl-porphyrin;
R_1=R_2=R_3=R_4=OH, namely: 5,10,15,20-tetra(4-hydroxyphenyl)-porphyrin.

Method for synthesis of 5-(4-hydroxyphenyl)-10,15,20-triphenyl-porphyrin (THPP). Benzaldehyde (20.1 mL, 196.8 mmol) and 4-hydroxybenzaldehyde (8.0 g, 65.6 mmol) were solved in 350 mL propionic acid, vigorously stirred and bring to reflux. A solution consisting of propionic acid (50 ml) and freshly distilled pyrrole (13.6 mL, 262.4 mmol) was added through a funnel during 40 minutes. After two hours, the reaction mixture was cooled and let to stay over night. The reaction mixture was washed with 600 mL hot water, filtered and washed again with excessive hot water giving rise to a mixture of dark-red colored porphyrins. Then the mixture was extracted in dichloromethane until the extracts are colorless. The solvent was evaporated and a mixture of porphyrins red colored in crystalline forms were obtained. HPLC and TLC analysis were performed and it has to be noticed that the mixture was formed from only five compounds (instead of six theoretically). The porphyrins were separated by column chromatography using as eluent the following mixture of solvents: dichloromethane/chloroform/methanol = 2/2/1-12/3/1. Each collected ring was further analyzed by TLC.

Porphyrin modified polysiloxane synthesis. The porphyrin modified polymers were obtained starting from a polysiloxane containing chlorobenzyl groups in the side-chain, according to the Scheme 2.

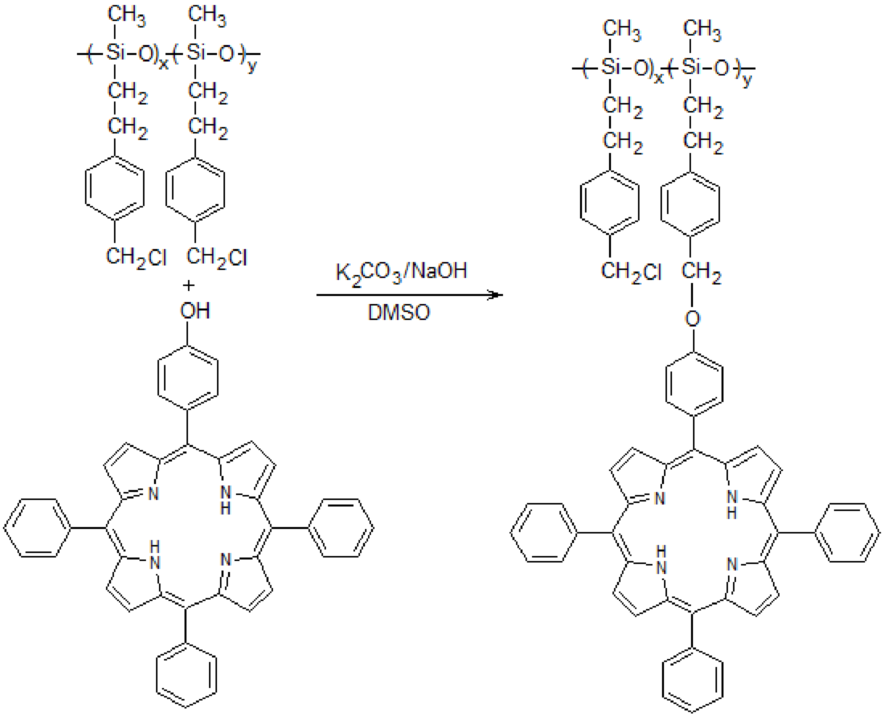

Scheme 2. Reaction scheme for the synthesis of the porphyrin modified polysiloxane

The polysiloxane with molecular weight between 5 and 6×10^{-3} were prepared by the hydrolytic polycondensation of [2-(4-chloromethylphenyl)ethyl]methyldichlorosilane. Details concerning polysiloxane synthesis and characterizations have been previously reported [5]. Porphyrin-containing polysiloxanes were prepared by the nucleophilic substitution on the chlorobenzyl groups. In a typical experiment, 0.3 g of the polysiloxane precursor was dissolved in 3 ml dimethylsulfoxide (DMSO) and mixed with 0.09g of THPP and 0.01g K_2CO_3. The mixture was heated at 80 ºC for 16 h. The resulting polymer was precipitated and washed several times with methanol to eliminate unreacted products before drying under vacuum.

Apparatus. FT-IR spectra were registered as KBr pellets on a Jasco 430 instrument in the 4000-400 cm^{-1} range. UV-visible spectra were recorded on a UV/VIS PERKIN ELMER, LAMBDA 12 spectrometer and on a JASCO UV-visible spectrometer, V-650 model. Fluorescence spectra were recorded in THF and in THF-aqueous systems on a Perkin Elmer Model LS 55 apparatus in a 1 cm cuvette. The HPLC analysis were performed on a JASCO apparatus equipped with KROMASIL SI 100 5 μm polar column, 240×4 mm with MD 1510 detector, at ambient temperature using UV detection at 420 nm. The samples were subjected to analysis (20 μl) at a flow rate of 1 mL/min using a mixture of solvents: dichloromethane/chloroform/methanol, as eluent for polar column. Solvent systems associated with chromatography are reported as v/v ratios. ^{1}H-NMR spectra were registered in $CDCl_3$ on a Bruker DRX 400 apparatus at 400 MHz. Proton chemical shifts, expressed in δ (ppm), were internally referenced to the residual proton resonance in $CDCl_3$ (δ 7.26). For MS analysis of porphyrin base a 212 Varian Finnigan Mat mass spectrometer was used.

The thermal analysis was performed by means of a Mettler Toledo TGA-SDTA851e device, in N_2 atmosphere, with a flow of 20 mL/min, a heating rate of 15 K/min and sample weight of 4–6 mg. DSC thermograms were recorded on a Mettler DSC12E calorimeter with a heating/cooling rate of 10 K/min.

Atomic force microscope (AFM) investigations were performed with a Nanosurf® EasyScan 2 Advanced Research AFM. All surface imaging measurements were done in ambient conditions with samples obtained onto a pure silica plate by slow evaporation of the solvent from a solution of the porphyrin or the polymer in THF. A stiff (450 μm × 50 μm × 2 μm) piezoelectric ceramic cantilever (spring constant of 0.2 N/m), with an integral tip oscillated near its resonance frequency of about 13 kHz was used in the measurements. AFM data are quantitative on all three dimensions, and were investigated in contact or tapping mode.

Spectroscopic studies. Absorption and fluorescence spectra were recorded at ambient temperature using 1 cm path length cells. The luminescence spectra were recorded at a 100 nm/min, with constant slit widths, for excitation (3 nm) and for emission (3.4 nm). Cut-off filters (390 nm or when proper 430nm) to eliminate harmonic or scattering peaks were used. For introducing basic and acidic conditions in THF solvent, stock aqueous solutions of 0.1 M NaOH and 0.1 M HCl were used. The pH values of the solutions were measured with a digital Radelkis pH-meter. *McIlvaine* buffer solutions of pH 2.5; 3.5 and 4.5 using disodium hydrogen phosphate and citric acid were made to verify the fluorescence sensor's measurements both for porphyrin-based and for porphyrin modified polysiloxane-based sensor.

Reagents. The reagents were provided of highest purity obtainable from Merck, Fluka and Scharlau and where is not specified, used without further purification. Other chemicals used in the sol-gel process were chloroform, dichloromethane, tetrahydrofuran, absolute ethanol, methanol, hydrochloric acid (HCl, 36%), all provided of Merck, and distilled water. Chloroform was stored over 4Å molecular sieves. Dichloromethane was distilled from CaH_2 under nitrogen. All aqueous solutions were prepared with distilled water. Thin-layer chromatography (TLC) was performed using Merck 60 F254 silica gel. Silica gel 60 (70–230 mesh, Merck) was used for column chromatography.

3. Results and discussion

The most important spectrometric analysis results that certify the structure of ***5-(4-hydroxyphenyl)-10,15,20-triphenyl-porphyrin (THPP)*** are given below**:** dark red crystals; yield: 8.8 %; mp over 320°C; ^{1}H-NMR ($CDCl_3$, 400MHz), δ, ppm: 9.92 (s, 1H, OH) 8.92-9.02 (bs, 8H, β-pyrrole), 8.29-8.32 (d, 6H, H-2,6 phenyl), 8.10-8.22 (d, 2H, H-2,6 phenyl), 7.90-7.94 (3 H, H-4 phenyl), 7.30-7.32 (d, 2H, H-3,5 phenyl), 7.22-7.26 (m, 6H, H-3,5 phenyl), -2.79 ppm (br s, 2H, internal-NH-pyrrole); FT-IR (KBr), cm^{-1}: 3443 (ν N-H), 3051 (ν C-H_{Ph}); 1611 and 1555 (ν C=C_{Ph}), 1509 (ν C=C_{ph}), 1470 (ν C=N); 1347 (ν C-N); 1216 (ν C-OH); 1168 (δ C-H_{Ph}), 1099 (δ C-H_{pyrrol}); 962 (δ C-H_{pyrrol}); 797 (γ C-H_{pyrrol}); 722, 699 (γ C-H_{ph}). UV-vis, THF (λ_{max} (log ε): 417.5(5.64), 514.0(4.29), 549.0(3.99), 592.0(3.74), 648.5(3.66). TLC (R_f chloroform/dichloromethane/methanol 5/5/1): 0.41; HPLC (acetone/toluene 1/1) (R_T, min): 3.093; MS (ESI$^+$): m/z=630.70 $M]^{+\cdot}$ ($[C_{44}H_{30}N_4O]^{+\cdot}$ molecular ion).

The bands displayed on the FT-IR spectrum of the THPP – base compound are attributed above, but the most important is the presence at 3419 cm^{-1} of a shoulder corresponding to OH group located on the broadened band attributed to N-H bond.

The UV-vis spectra of porphyrin (THPP) display *etio* type allure with the typical Soret band at 417.5 nm, and the four Q-bands in the visible region displaying absorption maxima around 514, 549, 592 and 648.5 nm, as presented in Figure 1. The Soret band is generated by the transition from a_{1u} (π) - e_g^* (π) and the other four Q bands correspond to a_{2u} (π) - e_g^* (π) transitions.

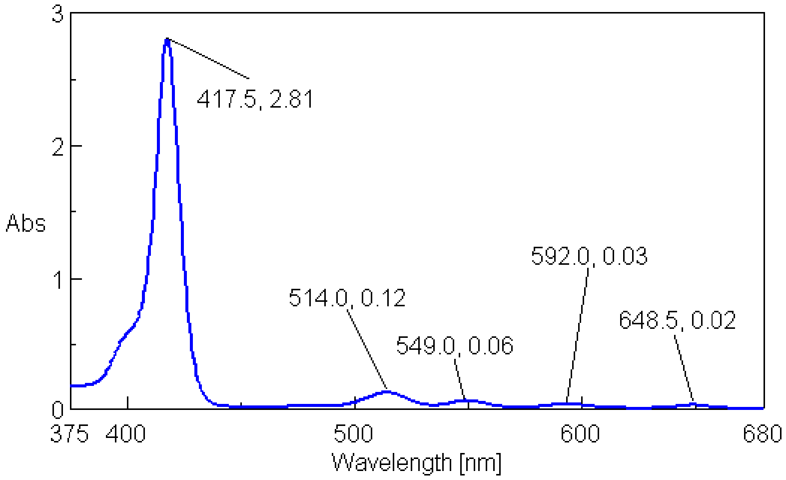

Fig. 1. The UV-vis spectrum of THPP in THF.

Previously reported data [24, 25] reveal that most of the porphyrin-bases manifest pronounced aggregation in acid aqueous solutions, accompanied by changes regarding the position, the shape and the intensity of the main absorption bands. In order to put into evidence the photophysical behavior of THPP we have investigated the absorption spectra of this porphyrin in THF-aqueous solution at different values of pH, as presented in Fig. 2.

By increasing acidity the protonation of the nitrogen atoms in the center of porphyrin ring is produced. The curve (2) from Fig. 2 shows a broadened Soret band, accompanied by a single Q band, which is the QI band, forbidden otherwise. The QI band is also bathochromic shifted from 648.5 nm (pH=5.5) to 669.5 nm (pH=3.5) and presents a significant hyperchromic effect.

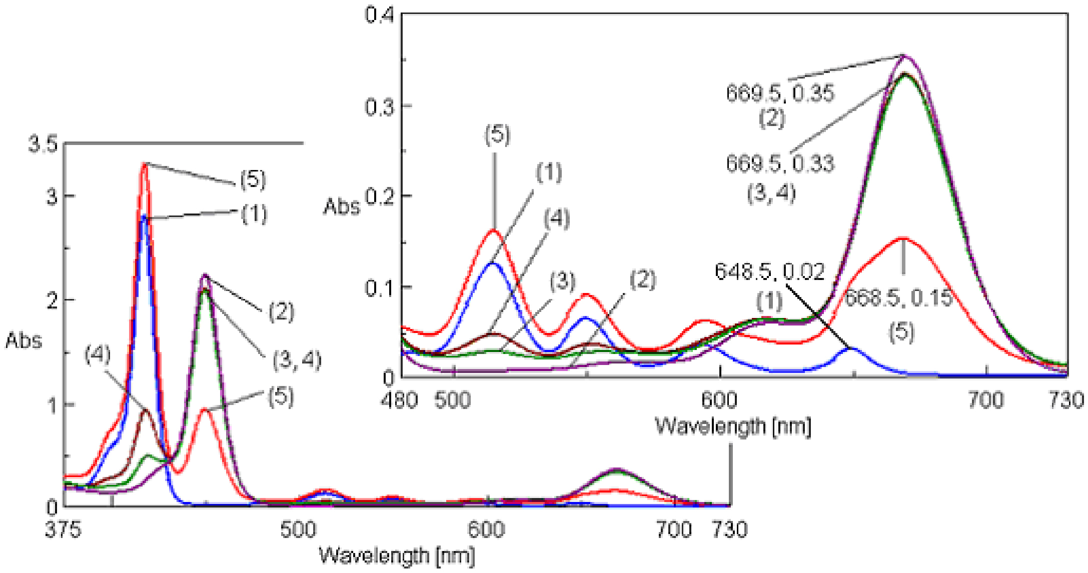

Fig. 2. The absorption spectra of porphyrin (THPP) in THF-aqueous solution in acid media: pH=5.5 (line 1); pH=3.5 (line 2); pH=3 (line 3); pH=2.5 (line 4); pH=1.5 (line5).

Upon increasing acidity of the solution, a clear tendency toward resolution is displayed by the splitting of the broadened Soret band into two individual Lorentzian bands located around 417 nm and 450 nm, respectively (Fig. 2, curve 2, 3, 4 and 5) as the result of the generation of aggregates. The band centered on 417 nm can be unequivocally assigned to the monomer. The presence of the isosbestic point around 430 nm is the proof of the existing equilibrium between the two species the monomer and the J aggregate. The second isosbestic point, putting into evidence the second type of protonated species is at 649 nm. The noticed decrease in the number of bands (Fig. 2, line 2 and 3) might be attributed to the increase of the D_{2h} symmetry of the porphyrin-base to D_{4h} corresponding to dication species.

A comparison between the UV-vis spectra of the solutions in THF of the pure porphyrin and of the polymer, offer only an insignificant difference of 1-2 nm of hypsochromic shift regarding the Soret and the Q II-IV bands of the polymer, as can be seen in Fig. 3.

Regarding the behavior of the new porphyrin modified polysiloxane in acid aqueous solutions it respects the shape and the positions of the bands displayed by bare porphyrin in Fig. 2, the difference consisting in the intensity of the bands, which is fourth times smaller for each band, if measured at the same concentration.

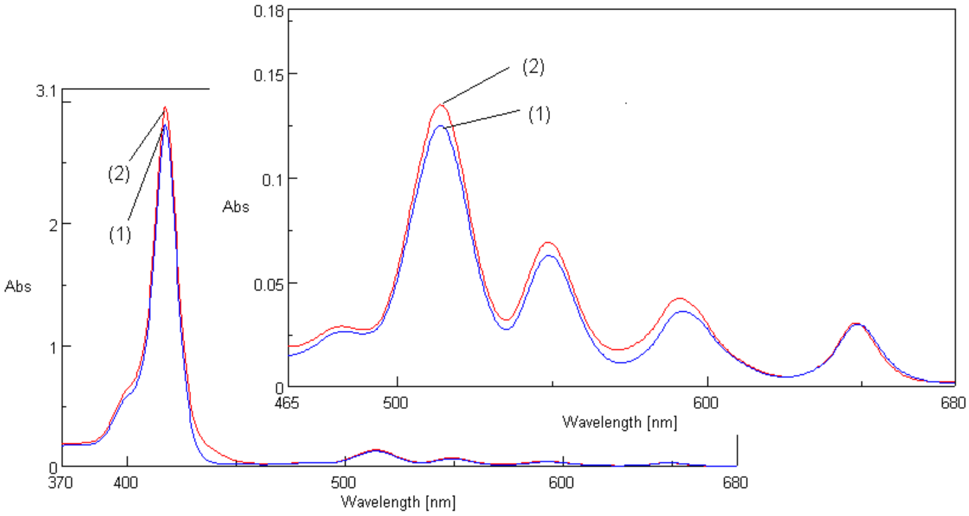

Fig. 3. Overlapped UV-vis spectra of the solution in THF of the pure porphyrin (line 1) and of the functionalized polymer (line 2).

The overlapped FT-IR spectra, of the porphyrin and of the functionalized polymer are displayed in Fig. 4.

Concerning the spectrum of the porphyrin-based polysiloxane one can identify together with the porphyrin signals, the characteristic signals reported usually in the literature [26] for the polysiloxanes, cm^{-1}: 799 (ν Si-C), 1020 and 1092 (ν Si-O-Si), 1262 (ν Si-CH_3), 2905 and 2960 (ν CH_3).

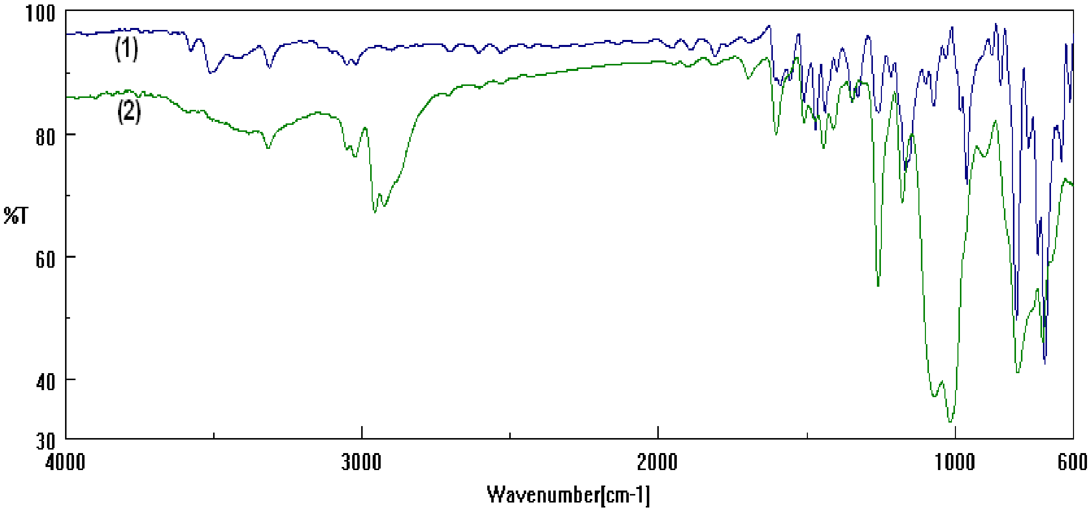

Fig. 4. Superposed FT-IR spectra (on MIRacle ATR accessory) of the porphyrin (line 1) and of the polymer (line 2).

The porphyrin-containing polysiloxane was characterized by ^{1}H-NMR spectroscopy and thermal analysis (DSC and thermo-gravimetric). In Fig. 5 are presented the unreacted and porphyrin-modified polysiloxanes NMR spectra.

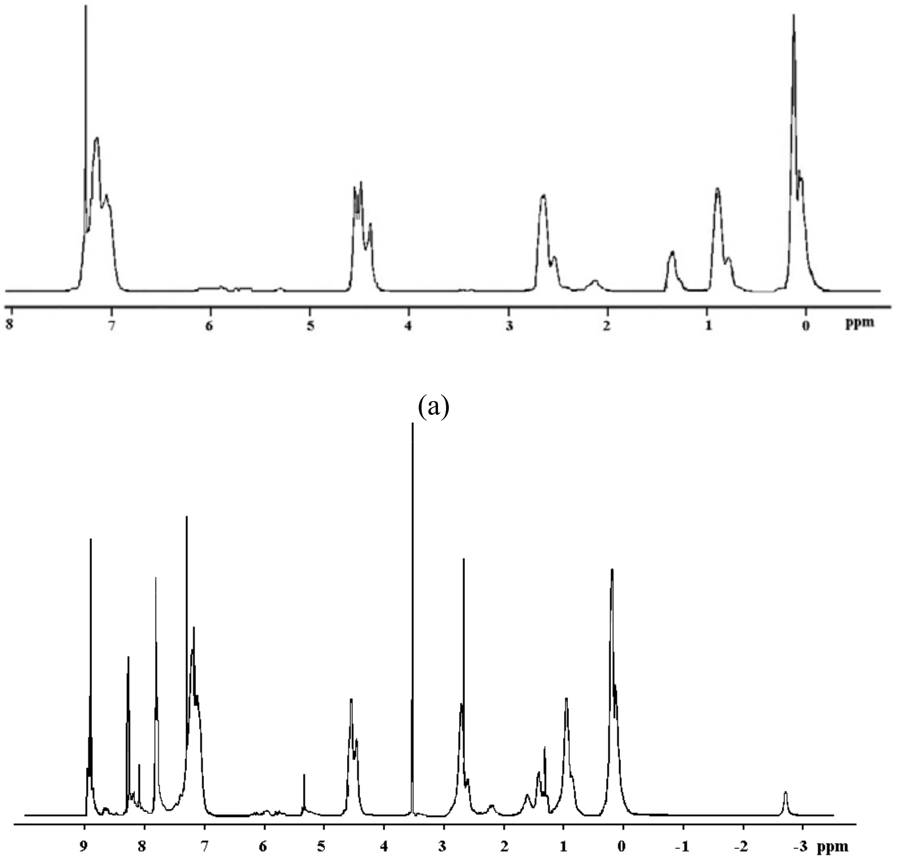

(a)

(b)

Fig. 5. The ^{1}H-NMR spectra corresponding to the unmodified polysiloxane (a) and porphyrin-modified polymer (b), respectively.

The specific signal corresponding to the porphyrin connection to the polysiloxanic chain is situated at 5.4 ppm (Fig. 5b). The substitution degree calculated based on this signal is 8.5 %. The other signals characteristic to the porphyrin group are present too, in the NMR spectrum. The molecular weight of the porphyrin-based polysiloxane, calculated taking into consideration the substitution degree is Mn = 7200.

The connection of the porphyrin group in the polysiloxanic side-chain is accompanied by a modification of the Tg value, that increase from -39 ºC (unmodified polysiloxane) to -20 ºC (porphyrin modified polysiloxane) – Fig. 6. This Tg modification also confirms the porphyrin connection on the polysiloxanic chain.

The porphyrin-based polymer has a good thermal stability, the degradation process beginning up to 300 ºC (Fig. 7). The TG curves profiles prove the existence of two degradation stages, the differences concerning the degradation domains supporting the idea of the porphyrin chemical connection in the side-chain.

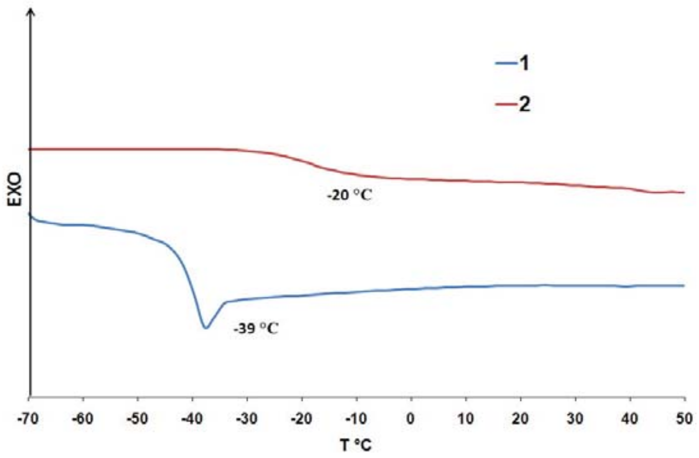

Fig. 6. DSC curves (second heating) corresponding to unmodified polysiloxane (1) and porphyrin-modified polymer (2) respectively.

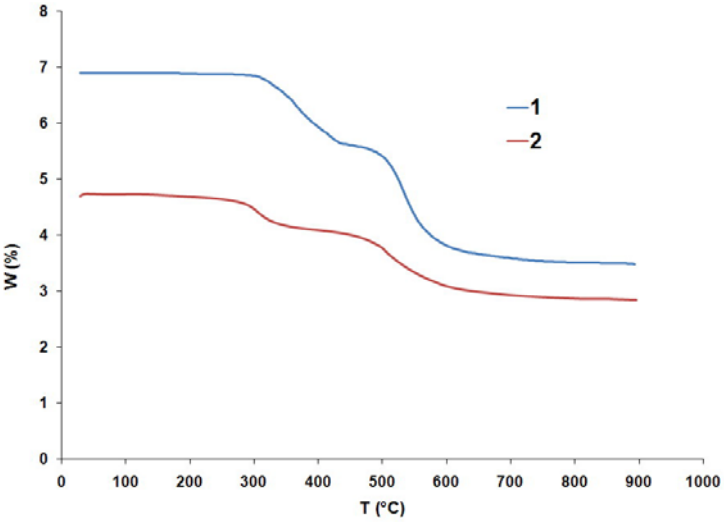

Fig. 7. The TG curves corresponding to unmodified polysiloxane (1) and porphyrin-modified polymer (2) respectively.

The emission spectra of bare THPP porphyrin in THF (Figure 8, line 1) exhibited two maxima, a strong and broad Q(0,0) fluorescence band at 654 nm, and a weaker emission band situated at 719 nm, assigned to Q(0,1) transition. The values of λ_{em} were obtained by exciting the samples at the wavelength of 415 nm.

The fluorescence spectra of the pure porphyrin were investigated in different acidic conditions and from Fig. 8, it is to be noticed that the position of the strong Q(0,0) bands is not changed but their corresponding intensity is continuously decreased with the increasing of the acidity (Fig. 8, lines1÷10, corresponding pH=5.5÷1.5).

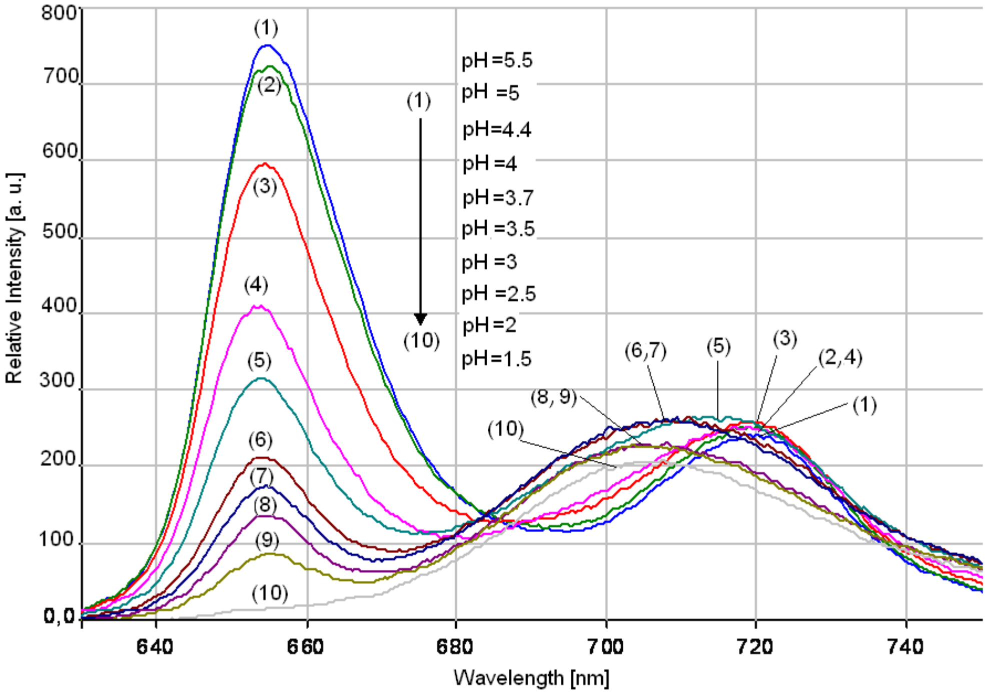

Fig. 8. The emission spectra of porphyrin (THPP) in THF-aqueous solution by varying the pH of acid media: pH=5.5 (line1) ÷ pH=1.5 (line10).

Although the position of the main emission band remain unchanged in the emission spectra of THPP by varying pH of the acid media, the position of the second band is hypsochromic shifted, moving from 719 nm (displayed in the interval of pH from 5.5÷3.7) to 706 nm (displayed in the interval of pH from 3.5÷1.5), but in the case of these bands the intensity does not suffer major modifications. Besides, the presence of two isosbestic points at 683 and 687 nm, indicates the presence of two equilibriums in the solution. The behavior of this porphyrin in acid media indicates the possibility of using it as a fluorescence pH sensor (Figure 9).

The dependence between the intensity of the main emission band of THPP measured at 655 nm and the pH of the environment is linear with a good correlation coefficient.

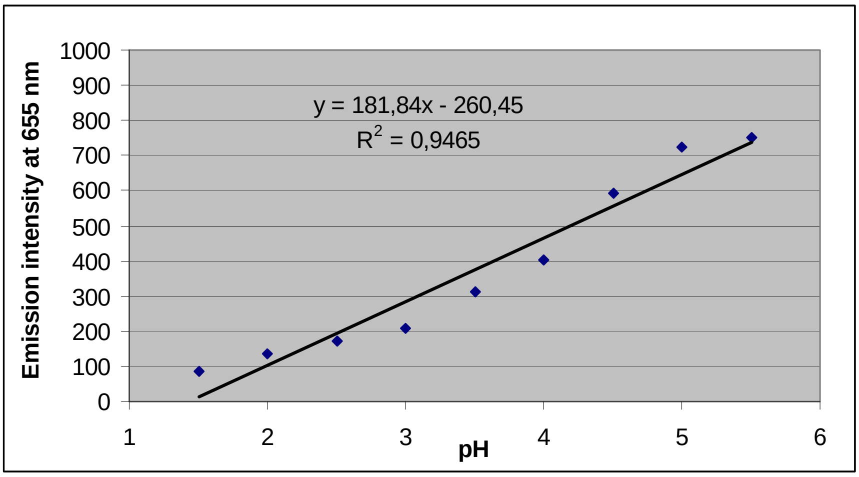

Fig. 9. The dependence between the intensity of the emission spectra of THPP measured at 655 nm and the pH of the environment.

In Figure 10 are presented the excitation and the emission spectra of the functionalized polymer, and the shape, position and the intensity of the bands are the same with that of the bare porphyrin.

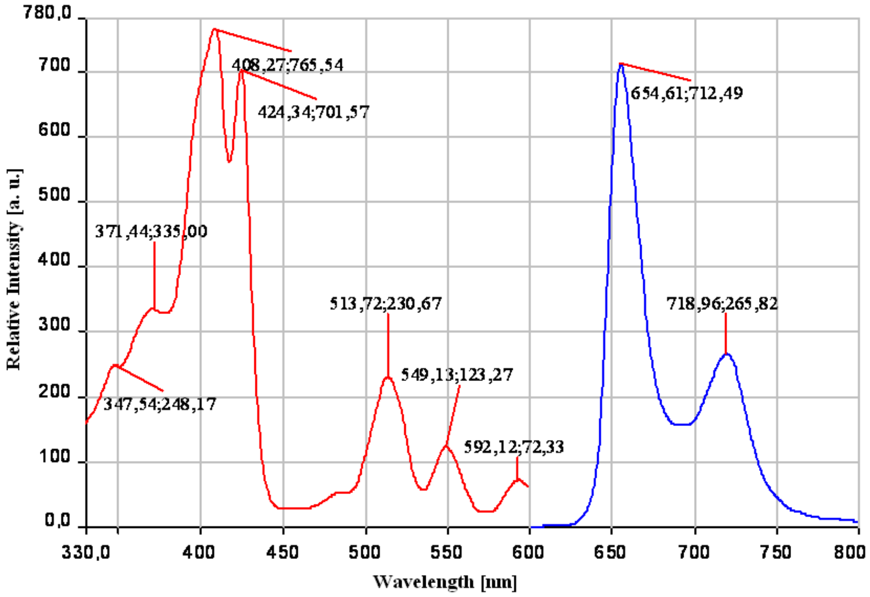

Fig. 10. Excitation (λ_{em}=655 nm, cut of filter 430 nm) and emission spectra (λ_{ex}=424 nm, cut of filter 430 nm) of the functionalized polymer in THF.

For a better view of this aspect, in Figure 11 a superposed image of the emission spectra of the porphyrin and of the functionalized polymer is displayed. The insignificant differences consist in a 1 nm hypsochromic shift of both bands of the polymer in comparison with the bands of the pure porphyrin and a small decrease of the intensity of the Q(0,0) fluorescence band with respect to the polymer.

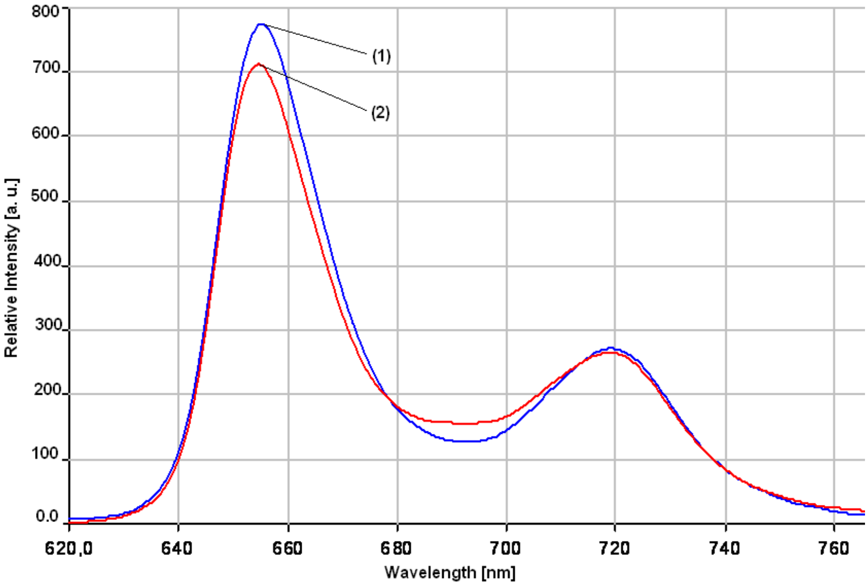

Fig. 11. Superposed emission spectra in THF of the bare porphyrin (line1) and of the functionalized polymer (line2).

The emission spectrum of the polymer was also investigated after 90 days to determine if a fluorescence quenching is registered (Figure 12).

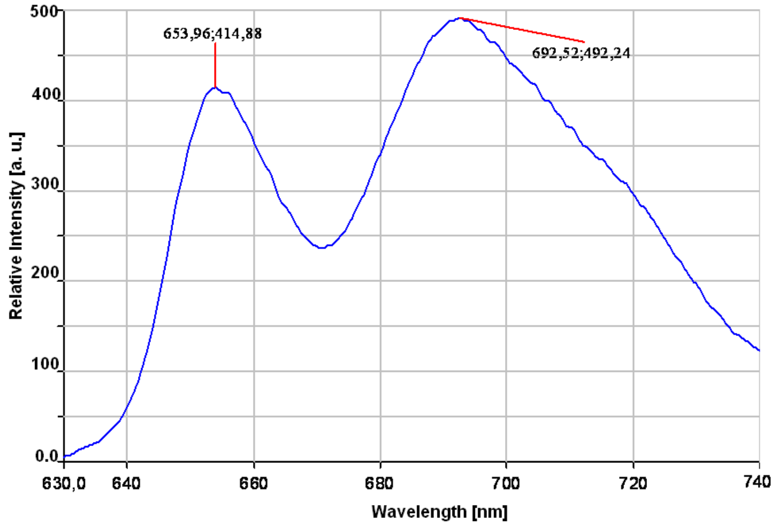

Fig. 12. The emission spectrum of the solution of the functionalized polymer in THF after 90 days.

As presented in Figure 12, the shape of the spectrum is totally changed, the Q(0,0) fluorescence band is only significant decreased in intensity, but the band assigned to Q(0,1) transition is hypsochromic shifted with 26 nm and is almost 100% increased in intensity, becoming the most important band.

In order to compare the luminescence behavior in acidic medium of the porphyrin grafted polysiloxane (Figure 13) with that of the bare porphyrin (Figure 8), the emission spectra were investigated by varying the value of pH, and from Figure 13, it is to be noticed that the position of the strong Q(0,0) bands is not changed but their corresponding intensity is continuously decreased with the increasing of acidity. As in case of pure porphyrin a linear dependence between the new polymer's intensity of the emission measured at 655 nm and the pH of the solution was established. The limits of the pH detection are narrower, but the confidence index is better (detail of Figure 13).

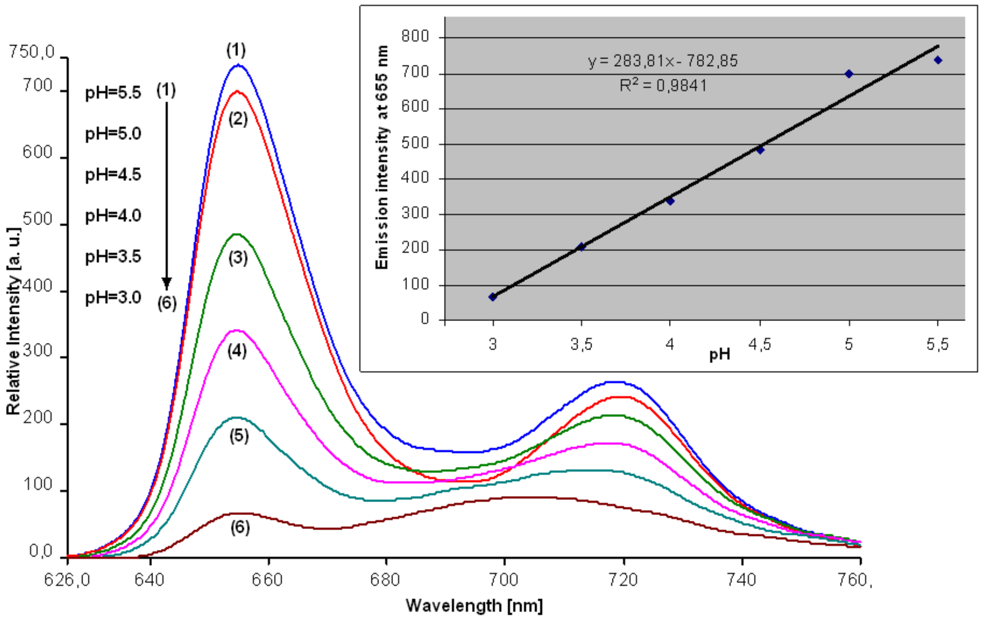

Fig. 13. The emission spectra of porphyrin modified polysiloxane in THF-aqueous solution by varying the pH of acid media: pH=5.5 (line 1) ÷ pH=3 (line 6). In detail the dependence between the intensity of the emission measured at 655 nm and the pH of the solution.

AFM analysis is a valuable technique to investigate the topography of the surfaces. From AFM measurements (more images for each sample) the following roughness parameters were finally analyzed, average surface roughness (Sa, *n*m); maximum peak height (Sp, *n*m); maximum valley depth (Sv, nm). In completion the diameter of the particles of the porphyrin and of the polymer was also estimated and besides, the number of islands and the mean surface of islands.

AFM measurements of the novel polymer reveal that the surface roughness (Sa) is increased from 0.4 nm, measured for the bare porphyrin (Figure 14), to 1.2 nm, measured for the polysiloxane grafted with porphyrin THPP (Figure 15).

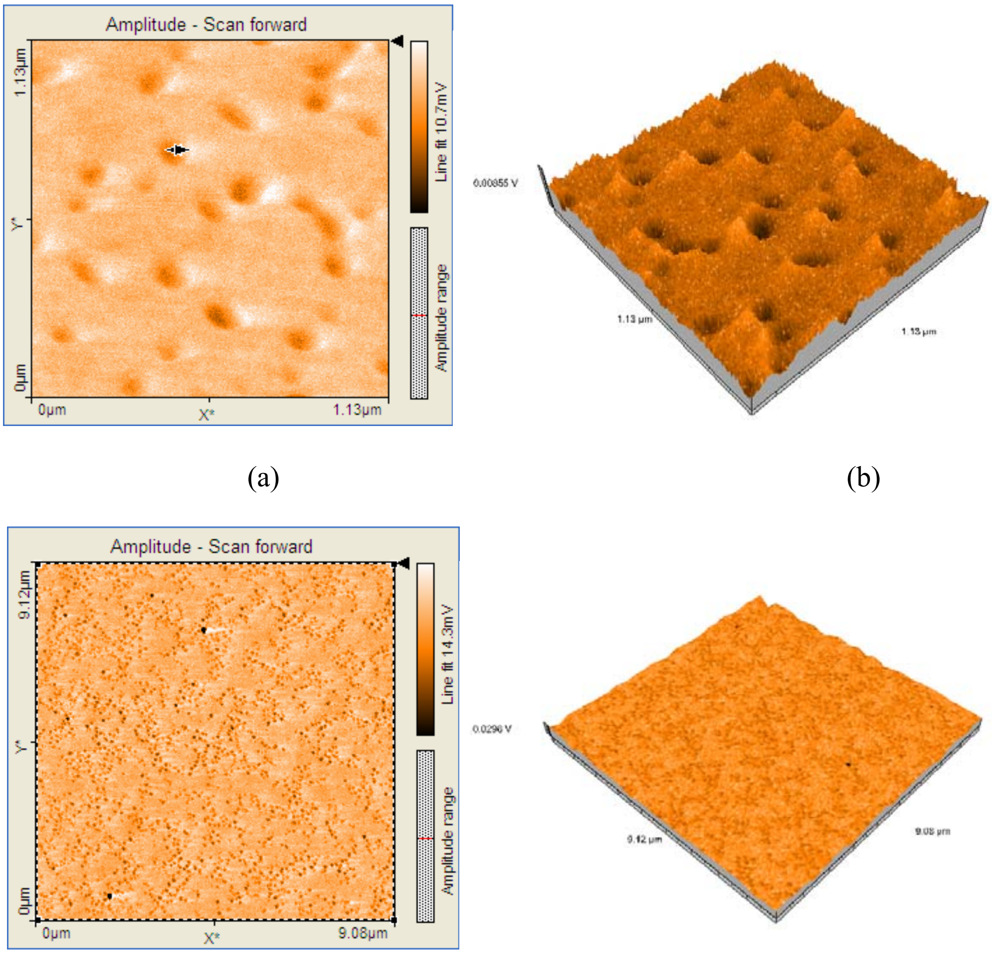

(a) (b)

(c) (d)

Fig. 14. 2D and 3D contact mode AFM of pure porphyrin (THPP) deposited on pure silica plates (1.13µm × 1.13 µm) (a) and (b); (9.08 µm × 9.08µm) (c) and (d).

The samples were formed by THF evaporation from a solution containing the porphyrin. In case of polymeric films obtained after the porphyrin macrocycles are grafted on side-chain of a polysiloxane it is possible to be generate some re-organization processes. As a consequence the reorganization of the material at its surface might give nano or micro-structured geometries.

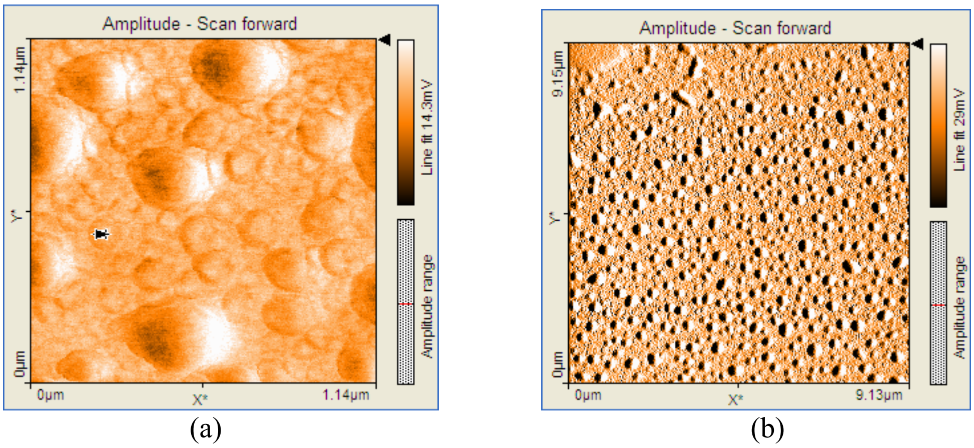

(a) (b)

Fig. 15. 2D tapping mode AFM of porphyrin-grafted on polysiloxane deposited as film on pure silica plates: 1.14µm × 1.14 µm (a) and 9.13 µm × 9.13µm (b).

The valley depth (Sv) is also deeper in case of polysiloxane material (– 9.2 nm) in comparison with a value of only -3.4 nm in case of porphyrin base. The peak height (Sp) is increasing from 2.8 nm on the surface of THPP to 7.4 nm on grafted polymer surface.

The spongeous structure of the functionalized polysiloxane material, with uniformly dispersed globular pores, might be explained by a oriented organization process, accompanied by a compression after releasing of the solvent (Figure 16).

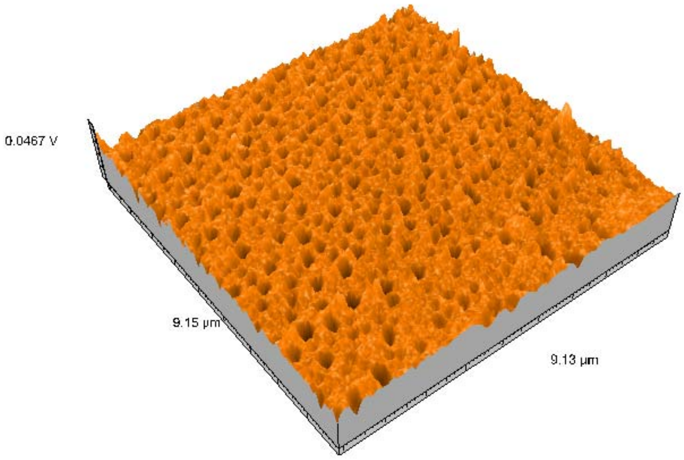

Fig. 16. 3D AFM image (aprox. 9 µm × 9 µm), of the porphyrin-grafted on polysiloxane (soft NanoSurf EasyScan2).

Regarding particle analysis, a comparison between the surfaces of porphyrin and the functionalized polymer with respect to the number of islands and the mean surface of islands reveal that on the same size analyzed aria, the porphyrin surface has almost six times more islands, but the surface of islands is almost two hundred times smaller.

Vesicular type morphology with particles ranging in diameter between 143.5 to 244 nm was put into evidence (Figure 15a). The particle size on the porphyrin surface is less than 82.5 nm in diameter (Figure 14a).

4. Conclusions

A new porphyrin modified polymer by the nucleophilic substitution on the chlorobenzyl groups of the side-chain of a polysiloxane by an asymmetrical mono-hydroxy-functionalized porphyrin, namely: 5-(4-hydroxyphenyl)-10,15,20-triphenyl-porphyrin (THPP) is reported. The porphyrin-containing polysiloxane was characterized by ^{1}H-NMR and FT-IR spectroscopy and thermal analysis (DSC and thermo-gravimetric), the obtained data confirming the porphyrin connection on the polysiloxanic chain and showing an increased thermal stability of the modified polymer. A comparison between optical absorption spectroscopy data and emission spectra of the bare porphyrin and of the polymer shows that the porphyrin-base polysiloxane preserves the optical properties of the porphyrinic dye. Both the pure porphyrin and the porphyrin modified polymer proved to be fluorescence pH sensors in acid domain. Atomic force microscopy (AFM) put into evidence a spongeous structure of the functionalized polysiloxane material, with uniformly dispersed globular pores, a topography that encourages to further application of this material in formulation of sensor devices. Besides, the presence of the band around 700 nm in the emission spectra of the porphyrin-grafted polysiloxane (very well preserved in time) gives hope in using it in photodynamic therapy of cancer (PDT).

Acknowledgement

Part of this work was obtained in the frame of Inter-academic Exchange Collaboration between Romanian Academy and Russian Academy of Sciences.

References

[1] J. Chojnowski, M. Cypryk, Synthesis of linear polysiloxanes, in: R.G. Jones, W. Ando, J. Chojnowski (Eds.), Silicon-Containing Polymers, Kluwer Academic Publishers, Dodrecht, pp. 3-42 (2000).

[2] S. Grigoras, in: J. Bicerano (Ed.), Computational Modeling of Polymers, M. Dekker, New York, p. 161 (1993).

[3] J. Chojnowski, in: S.J. Clarson, J.A. Semlyen (Eds.), Siloxane Polymers, Prentice Hall, Englewood Cliffs, New Jersey, p. 1 (1993).

[4] S.Y. Pyun, W.G. Kim, Macromol. Res. **11**, 202 (2003).

[5] K. Kazmierski, N. Hurduc, G. Sauvet, J. Chojnowski, J. Polym. Sci. Part A: Polym. Chem. **42**, 1682 (2004).

[6] J. Zimmermann, M. Rabe, D. Verdes, S. Seeger, Langmuir **24**, 1053 (2008).

[7] C.A. Bradley, B.D. Yuhas, M.J. McMurdo, T. Don Tilley, Chem. Mater. **21**, 174 (2009).

[8] U. Singh, C. Hunte, H. Gleeson, Liq. Cryst. **28**, 697 (2001).

[9] J.P. Xu, J. Ji, X.L. Wang, J.C. Shen, J. Mater. Sci. - Mater. Med. **16**, 277 (2005).

[10] C. Monnereau, E. Blart, V. Montembault, L. Fontaine, F. Odobel, Tetrahedron **61**, 10113 (2005).

[11] D. Wróbel, A. Siejak, P.Ław Siejak, Sol. Energy Mater. Sol. Cells **94**, 492 (2010).

[12] E. Girgenti, R. Ricoux, J.P. Mahy, Tetrahedron **60**, 10049 (2004).

[13] M.A. García-Sánchez, V. De la Luz, M.L. Estrada-Rico, M.M. Murillo-Martínez, M.I. Coahuila-Hernández, R. Sosa-Fonseca, S.R. Tello-Solís, F. Rojas, A. Campero, J. Non-Cryst. Solids **355**, 120 (2009).

[14] G. Li, S. Bhosale, S. Tao, R. Guo, S. Bhosale, F. Li, Y. Zhang, T. Wang, J.H. Fuhrhop, Polymer **46**, 5299 (2005).

[15] A. Bartczak, Y. Namiki, D.J. Qian, J. Miyake, A. Boguta, J. Goc, J. Łukasiewicz, D. Frackowiak, J. Photochem. Photobiol., A **159**, 259 (2003).

[16] G.D. Zhang, A. Harada, N. Nishiyama, D.L. Jiang, H. Koyama, T. Aida, K. Kataoka, J. Controlled Release **93**, 141 (2003).

[17] Y. Amao, T. Miyashita, I. Okura, J. Fluorine Chem. **107**, 101 (2001).

[18] K.T. Nielsen, H. Spanggaard, F.C. Krebs, Displays **25**, 231 (2004).

[19] T. Shimidzu, H. Segawa, F. Wu, N. Nakayama, J. Photochem. Photobiol., A **92**, 121 (1995).
[20] A.D. Adler, F.R. Longo, J. Goldmacher, J. Assour, L. Korsakoff, J. Org. Chem. **32**, 476 (1967).
[21] L. Xiangqing, W. Xingoiao, S. Yingyan, G. Jingfu, D. Jiangwen, L. Guofa, Chemistry Mag. Org. **3**, 37 (2001).
[22] Z. Jing, G. Yang, C. Shaokui, Z. Wennan, W. Dongmei, C. Huifang, L. Tianxuan, Chemistry Mag. Org. **8**, 39 (2002).
[23] E. Fagadar-Cosma, B. Maranescu, C. Enache, C. Savii, G. Fagadar-Cosma, Rev. Chim. **57**, 1144 (2006).
[24] E. Fagadar-Cosma, L. Cseh, V. Badea, G. Fagadar-Cosma, D. Vlascici, Comb. Chem. High Throughput Screening **10**, 466 (2007).
[25] E. Fagadar-Cosma, C. Enache , I. Armeanu, D. Dascalu, G. Fagadar-Cosma, M. Vasile, I. Grozescu, Mater. Res. Bull. **44**, 426 (2009).
[26] D. Bodas, C. Khan-Malek, Microelectron. Eng. **83**, 1277 (2006).